BNL-101426-2014-TECH

RHIC/RF- 7;BNL-101426-2013-IR

Scanning of the interaction-point consequences for the RHIC storage RF system

W. Pirki

April 1993

Collider Accelerator Department

Brookhaven National Laboratory

U.S. Department of Energy

USDOE Office of Science (SC)

DISCLAIMER

Scanning of the Interation-Point:

Consequences for the RHIC Storage

RF System

Werner Pirkl

Brookhaven National Laboratory
April 1993

Introduction

The RHIC storage rf system consists of six common cavities in the inter-action region (acting on both beams simultaneously), complemented by two individual cavities per ring (acting on a single beam). The beams are supposed to traverse the cavity gaps at the zero crossing of the rf voltage, such that there is longitudinal focussing but no energy gain.

This condition can be met for both beams simultaneously as long as their interaction point is located at the midplane of the common cavity group (or an integer multiple of halfwaves away). Scanning of the interaction point for detector calibration breaks the geometrical symmetry with respect to the cavity assembly and leads to phase errors that have to be compensated by the individual cavities.

This note discusses the consequences for the layout of the storage rf system and gives practical limits for the extent of the interaction point scan.

Beam phases in the common cavity group

The space-time diagram of fig 1 depicts the phase relationships:

- the abscissa represents distances, in particular the positions of the cavities. They are grouped in pairs, arranged symmetrically around the nominal interaction point at equal intervals of lambda/2 and fed with alternating polarities. Three cavity pairs are shown, with the first possible cavity pair location near to the interaction point left empty. The cavities may also be further pushed apart to increase the space available for a particle detector.

-the ordinate represents time, expressed in units of the rf period; the actual rf waveshape of the cavities is also shown. The lines under 45 degrees correspond to two sets of beams running with speed of light in alternate directions; full lines refer to the beams crossing at the nominal interaction point, broken lines to the beams crossing lambda/16 to the right of that symmetry point.

It can be seen that both beams colliding at the nominal interaction point will both traverse the cavity gaps at zero crossing of the rf waveshape. Also the absolute voltage slopes are of different sign, their focussing effect on both beams is the same since the particles traverse the gap with opposite directions (and hence undergo rf forces of opposite sign).

Beams colliding at some distance from the nominal interaction point will experience non-zero rf voltage at their center. As can be seen from fig.1, both beams will encounter a voltage of the same magnitude and polarity at each cavity. Owing to the different beam directions, one of the beams will be subject to systematic net energy gain, the other to net energy loss. This has to be compensated by the individual cavities of each ring in order to keep the beam energy and hence beam orbits constant.

Beam loading in the common cavities.

Fig.2 shows the conditions on cavity 3D in the time domain together with a phasor diagram. Beam 1 extracts, beam 2 restores energy, on the average the net energy flow cancels out. Beam loading is purely reactive, of magnitude

$$IR = 2 * IB1 * COS(PHI),$$

where IB1 is the rf beam current in a single ring and

$$PHI = 2 * PI * L / LAMBDA$$

the rf phase corresponding to the geometric beam offset L from the nominal interaction point. Note that the reactive beam loading is largest for nominal beam position (L = PHI = 0), an illustration of the fact that the rf focussing is also strongest there.

Beam loading in the individual cavities.

The power to be delivered by the individual cavities increases with the amount of geometrical beam offset L from the nominal interaction point. Even for infinite available

power there exists a hard limit for the maximum possible phase deviation PHIMAX of the beam, namely the phase at which the full available voltage of the individual cavities is used to re-establish quadrature between beam and overall combined voltage, see fig 3.

$$PHIMAX = ASIN(NCAV.IND/NCAV.COM) = ASIN(2/6) = 0.3398$$

The maximum geometric deviation LMAX follows from

$$LMAX = PHIMAX * LAMBDA /(2 * PI) = 82.7\ mm$$

The phasor diagram for phase deviations smaller than PHIMAX at a cavity that has restore (rather then sink) beam energy is shown in fig 4.

It is supposed that the cavity tuner remained in the optimum position for zero beam offset due to the anticipated rapidity of the scan. The amplifier has to deliver a sizeable additional rf current which ultimately hits the limits of the power tube and/or the DC power supply. Numerical values of several key parameters are listed in the annex as a function of beam offset, for both the accelerating and the decelerating cavities.

The limiting value in the present case is the peak current capability of the amplifier tube. The amplifier has been tested at CERN for peak cathode currents up to about 60 A; the unit can no longer be operated CW but has to be pulsed, at 20% maximum duty factor and pulses of max. 1 sec duration.

That limiting peak cathode current of 60 A corresponds to a beam offset of about +64 mm. The combined rf voltage URF.STO is reduced to 7.05 MV under these conditions, the DC supply current in an accelerating amplifier attains 16.8 A, the necessary rf drive power 5.2 kW.

The decelerating counterpart in the other ring draws a DC current of only 3.83 A for the same (negative) beam offset. If the scan of the interaction point is rapid and double-sided, such that the individual cavities of a ring are alternating acceleration and deceleration in sufficiently fast sequence, then the currents for the two modes can be averaged in a storage capacitor and the requirements on the power supply remain essentially unchanged.

Conclusion

A maximum beam offset of about +-64 mm can be achieved at 20% duty factor for pulse length of 1 second. The peak cathode current of the final rf amplifier is the limiting factor. Amplifier drive chain and DC power supply have to be designed with considerable

reserve to attain these limits. If the scan cycle is fast and symmetric (i.e. upstream/downstream of the interaction point) the power supply requirements can be significantly reduced.

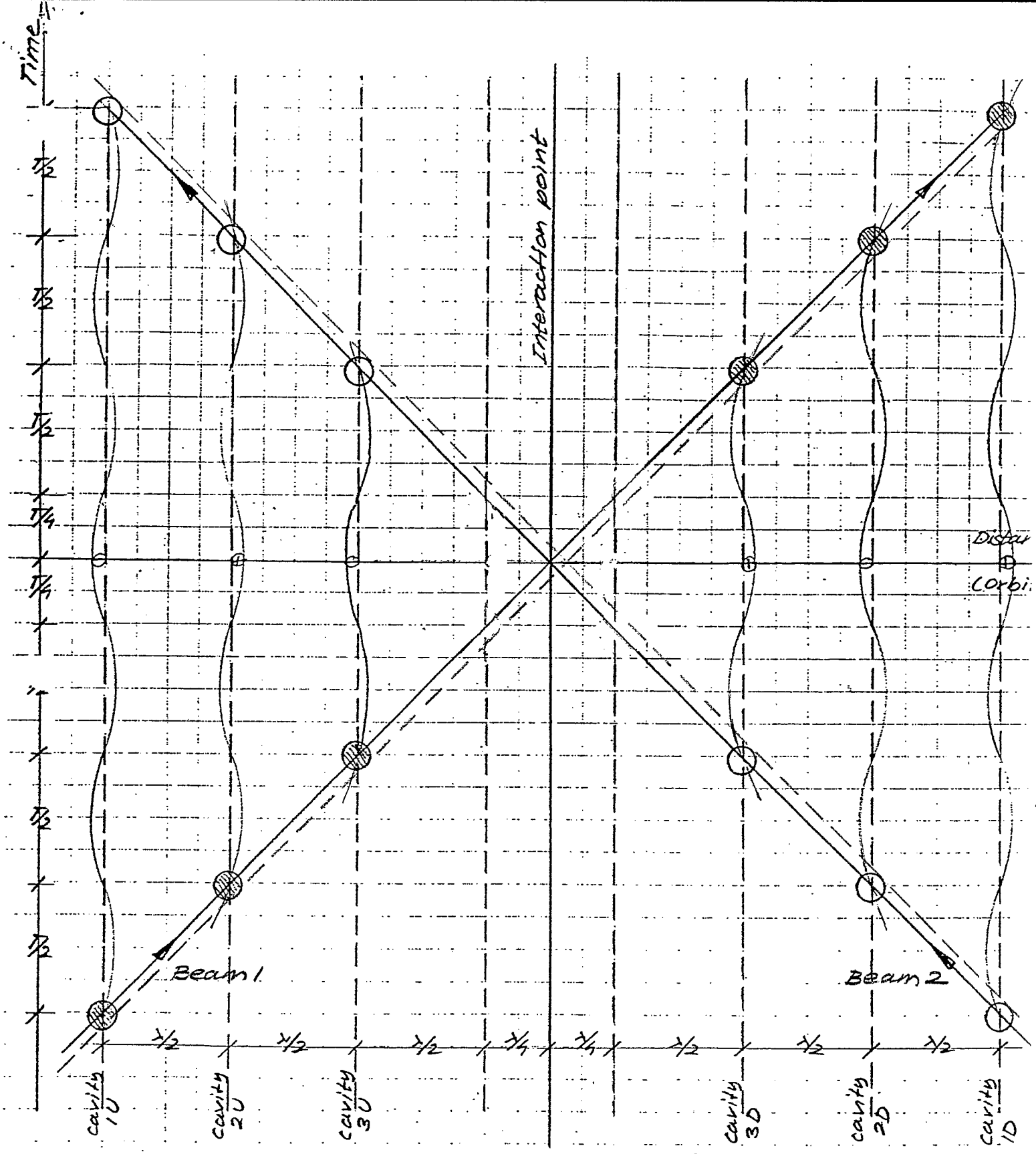

FIG 1:
PHASING OF CAVITIES
IN INTERACTION REGION

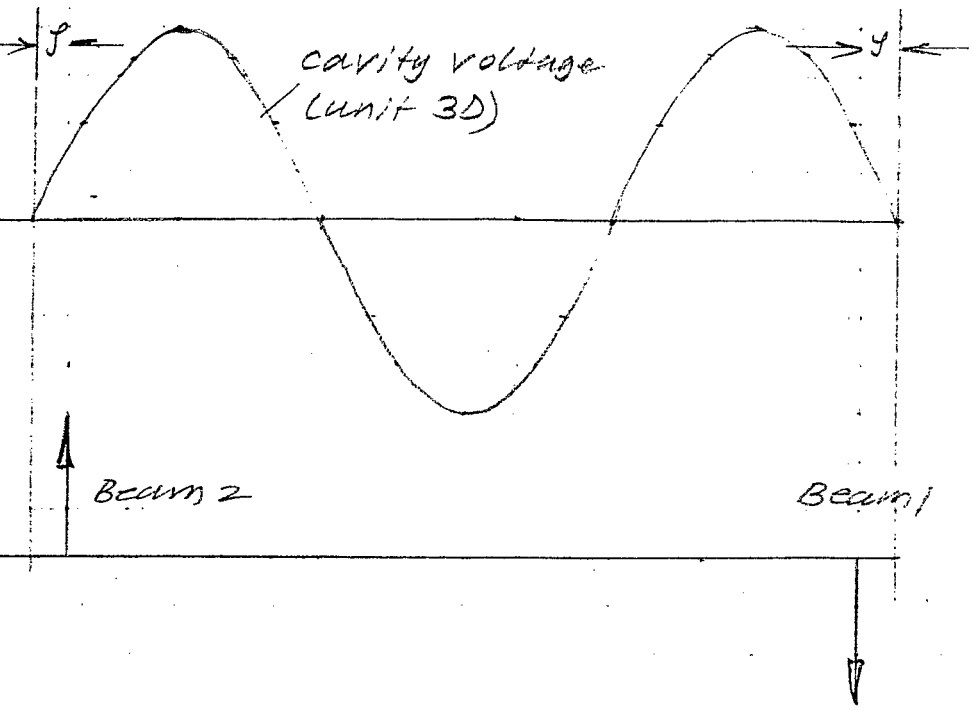

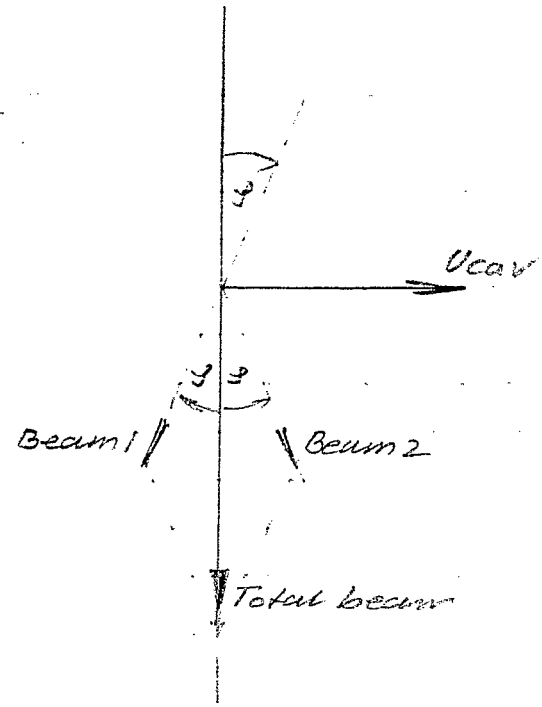

Fig 2: Beam load at common cavities

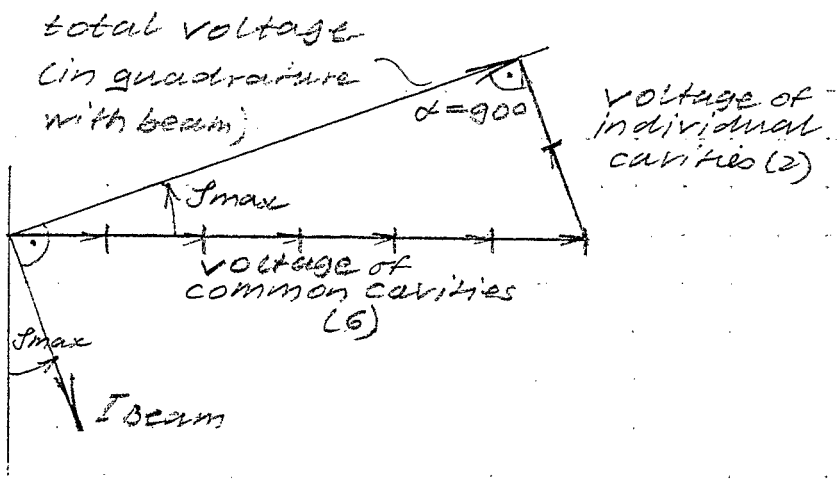

Fig 3: Maximum possible dephasing

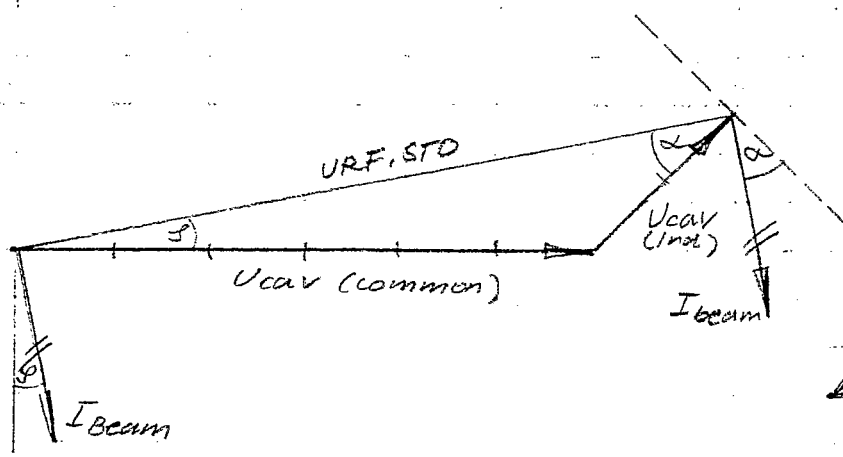

Fig 4A: Phase relation between common and individual cavities
$\varphi < \varphi_{max}$, $\alpha < 90°$

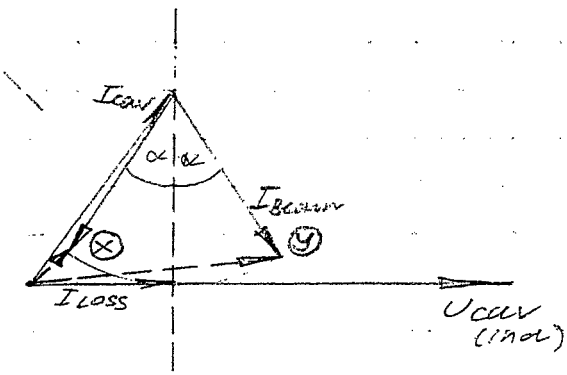

Fig 4B: Voltage and current in individual cavity
– – – amplifier current
⊗ decelerating Ⓨ accelerating

ANNEX

frf	1.961E+08	** RF frequency
urf.cav	1000000	** Cavity RF voltage
pcav	60000	** Cavity RF power
ibeam	.14	** RF beam current
urf.amp	8500	** Amplifier RF voltage
udc.amp	10000	** Amplifier DC voltage
idc.ipp	.278	** Tube class-B ratio Idc/Ipeak
irf.ipp	.457	** Tube class-B ratio Irf/Ipeak
ncav.com	6	** Number of common cavities
ncav.ind	2	** Number of individual cavities

L	PHI.deg	ALFA.deg	URF.STO	IPP	Idc	PRF	PDISS
2.00E-03	47.1E-02	14.1E-01	80.0E+05	31.8E+00	88.3E-01	61.7E+03	26.6E+03
4.00E-03	94.2E-02	28.3E-01	80.0E+05	32.7E+00	90.8E-01	63.5E+03	27.4E+03
6.00E-03	14.1E-01	42.4E-01	79.9E+05	33.6E+00	93.3E-01	65.2E+03	28.1E+03
8.00E-03	18.8E-01	56.6E-01	79.9E+05	34.4E+00	95.8E-01	66.9E+03	28.9E+03
1.00E-02	23.5E-01	70.8E-01	79.8E+05	35.3E+00	98.2E-01	68.6E+03	29.6E+03
1.20E-02	28.2E-01	85.0E-01	79.7E+05	36.2E+00	10.1E+00	70.3E+03	30.3E+03
1.40E-02	33.0E-01	99.3E-01	79.6E+05	37.1E+00	10.3E+00	72.1E+03	31.1E+03
1.60E-02	37.7E-01	11.4E+00	79.5E+05	38.0E+00	10.6E+00	73.8E+03	31.8E+03
1.80E-02	42.4E-01	12.8E+00	79.3E+05	38.9E+00	10.8E+00	75.5E+03	32.6E+03
2.00E-02	47.1E-01	14.3E+00	79.2E+05	39.8E+00	11.1E+00	77.2E+03	33.4E+03
2.20E-02	51.8E-01	15.7E+00	79.0E+05	40.7E+00	11.3E+00	79.0E+03	34.1E+03
2.40E-02	56.5E-01	17.2E+00	78.8E+05	41.6E+00	11.6E+00	80.7E+03	34.9E+03
2.60E-02	61.2E-01	18.7E+00	78.6E+05	42.5E+00	11.8E+00	82.4E+03	35.7E+03
2.80E-02	65.9E-01	20.1E+00	78.4E+05	43.4E+00	12.1E+00	84.1E+03	36.4E+03
3.00E-02	70.6E-01	21.6E+00	78.1E+05	44.3E+00	12.3E+00	85.8E+03	37.2E+03
3.20E-02	75.3E-01	23.2E+00	77.9E+05	45.2E+00	12.6E+00	87.5E+03	38.0E+03
3.40E-02	80.0E-01	24.7E+00	77.6E+05	46.1E+00	12.8E+00	89.2E+03	38.8E+03
3.60E-02	84.7E-01	26.2E+00	77.3E+05	47.0E+00	13.1E+00	90.9E+03	39.6E+03
3.80E-02	89.5E-01	27.8E+00	77.0E+05	47.9E+00	13.3E+00	92.7E+03	40.5E+03
4.00E-02	94.2E-01	29.4E+00	76.6E+05	48.8E+00	13.6E+00	94.4E+03	41.3E+03
4.20E-02	98.9E-01	31.0E+00	76.3E+05	49.7E+00	13.8E+00	96.1E+03	42.2E+03
4.40E-02	10.4E+00	32.6E+00	75.9E+05	50.7E+00	14.1E+00	97.8E+03	43.1E+03
4.60E-02	10.8E+00	34.3E+00	75.5E+05	51.6E+00	14.3E+00	99.5E+03	44.0E+03
4.80E-02	11.3E+00	36.0E+00	75.0E+05	52.5E+00	14.6E+00	10.1E+04	44.9E+03
5.00E-02	11.8E+00	37.7E+00	74.6E+05	53.5E+00	14.9E+00	10.3E+04	45.8E+03
5.20E-02	12.2E+00	39.5E+00	74.1E+05	54.4E+00	15.1E+00	10.5E+04	46.8E+03
5.40E-02	12.7E+00	41.3E+00	73.6E+05	55.4E+00	15.4E+00	10.6E+04	47.8E+03
5.60E-02	13.2E+00	43.2E+00	73.0E+05	56.4E+00	15.7E+00	10.8E+04	48.9E+03
5.80E-02	13.7E+00	45.1E+00	72.4E+05	57.4E+00	16.0E+00	11.0E+04	50.0E+03
6.00E-02	14.1E+00	47.1E+00	71.8E+05	58.4E+00	16.2E+00	11.1E+04	51.2E+03
6.20E-02	14.6E+00	49.1E+00	71.2E+05	59.5E+00	16.5E+00	11.3E+04	52.4E+03
6.40E-02	15.1E+00	51.2E+00	70.5E+05	60.5E+00	16.8E+00	11.5E+04	53.6E+03
6.60E-02	15.5E+00	53.5E+00	69.7E+05	61.6E+00	17.1E+00	11.6E+04	55.0E+03
6.80E-02	16.0E+00	55.8E+00	68.9E+05	62.7E+00	17.4E+00	11.8E+04	56.5E+03
7.00E-02	16.5E+00	58.3E+00	68.0E+05	63.9E+00	17.8E+00	12.0E+04	58.1E+03
7.20E-02	16.9E+00	61.0E+00	67.1E+05	65.1E+00	18.1E+00	12.1E+04	59.8E+03
7.40E-02	17.4E+00	63.9E+00	66.0E+05	66.4E+00	18.5E+00	12.3E+04	61.7E+03
7.60E-02	17.9E+00	67.2E+00	64.9E+05	67.8E+00	18.8E+00	12.5E+04	64.0E+03
7.80E-02	18.4E+00	70.9E+00	63.5E+05	69.3E+00	19.3E+00	12.6E+04	66.6E+03
8.00E-02	18.8E+00	75.6E+00	61.8E+05	71.1E+00	19.8E+00	12.8E+04	70.0E+03
8.20E-02	19.3E+00	82.6E+00	59.2E+05	73.7E+00	20.5E+00	12.9E+04	75.4E+03

(A) Accelerating cavity

ANNEX

frf	1.961E+08	** RF frequency
urf.cav	1000000	** Cavity RF voltage
pcav	60000	** Cavity RF power
ibeam	.14	** RF beam current
urf.amp	8500	** Amplifier RF voltage
udc.amp	10000	** Amplifier DC voltage
idc.ipp	.278	** Tube class-B ratio Idc/Ipeak
irf.ipp	.457	** Tube class-B ratio Irf/Ipeak
ncav.com	6	** Number of common cavities
ncav.ind	2	** Number of individual cavities

L	PHI.deg	ALFA.deg	URF.STO	IPP	Idc	PRF	PDISS
-2.00E-03	-47.1E-02	-14.1E-01	80.0E+05	30.0E+00	83.4E-01	58.3E+03	25.1E+03
-4.00E-03	-94.2E-02	-28.3E-01	80.0E+05	29.1E+00	80.9E-01	56.5E+03	24.4E+03
-6.00E-03	-14.1E-01	-42.4E-01	79.9E+05	28.2E+00	78.5E-01	54.8E+03	23.6E+03
-8.00E-03	-18.8E-01	-56.6E-01	79.9E+05	27.3E+00	76.0E-01	53.1E+03	22.9E+03
-1.00E-02	-23.5E-01	-70.8E-01	79.8E+05	26.5E+00	73.5E-01	51.4E+03	22.2E+03
-1.20E-02	-28.2E-01	-85.0E-01	79.7E+05	25.6E+00	71.1E-01	49.7E+03	21.4E+03
-1.40E-02	-33.0E-01	-99.3E-01	79.6E+05	24.7E+00	68.6E-01	47.9E+03	20.7E+03
-1.60E-02	-37.7E-01	-11.4E+00	79.5E+05	23.8E+00	66.2E-01	46.2E+03	20.0E+03
-1.80E-02	-42.4E-01	-12.8E+00	79.3E+05	22.9E+00	63.7E-01	44.5E+03	19.2E+03
-2.00E-02	-47.1E-01	-14.3E+00	79.2E+05	22.0E+00	61.3E-01	42.8E+03	18.5E+03
-2.20E-02	-51.8E-01	-15.7E+00	79.0E+05	21.2E+00	58.9E-01	41.0E+03	17.8E+03
-2.40E-02	-56.5E-01	-17.2E+00	78.8E+05	20.3E+00	56.5E-01	39.3E+03	17.1E+03
-2.60E-02	-61.2E-01	-18.7E+00	78.6E+05	19.5E+00	54.1E-01	37.6E+03	16.5E+03
-2.80E-02	-65.9E-01	-20.1E+00	78.4E+05	18.6E+00	51.7E-01	35.9E+03	15.8E+03
-3.00E-02	-70.6E-01	-21.6E+00	78.1E+05	17.8E+00	49.4E-01	34.2E+03	15.3E+03
-3.20E-02	-75.3E-01	-23.2E+00	77.9E+05	17.0E+00	47.2E-01	32.5E+03	14.7E+03
-3.40E-02	-80.0E-01	-24.7E+00	77.6E+05	16.2E+00	45.0E-01	30.8E+03	14.2E+03
-3.60E-02	-84.7E-01	-26.2E+00	77.3E+05	15.4E+00	42.8E-01	29.1E+03	13.8E+03
-3.80E-02	-89.5E-01	-27.8E+00	77.0E+05	14.7E+00	40.8E-01	27.3E+03	13.5E+03
-4.00E-02	-94.2E-01	-29.4E+00	76.6E+05	14.0E+00	38.9E-01	25.6E+03	13.3E+03
-4.20E-02	-98.9E-01	-31.0E+00	76.3E+05	13.4E+00	37.1E-01	23.9E+03	13.2E+03
-4.40E-02	-10.4E+00	-32.6E+00	75.9E+05	12.8E+00	35.6E-01	22.2E+03	13.3E+03
-4.60E-02	-10.8E+00	-34.3E+00	75.5E+05	12.3E+00	34.2E-01	20.5E+03	13.6E+03
-4.80E-02	-11.3E+00	-36.0E+00	75.0E+05	11.9E+00	33.1E-01	18.9E+03	14.2E+03
-5.00E-02	-11.8E+00	-37.7E+00	74.6E+05	11.6E+00	32.3E-01	17.2E+03	15.1E+03
-5.20E-02	-12.2E+00	-39.5E+00	74.1E+05	11.5E+00	31.8E-01	15.5E+03	16.4E+03
-5.40E-02	-12.7E+00	-41.3E+00	73.6E+05	11.4E+00	31.8E-01	13.8E+03	18.0E+03
-5.60E-02	-13.2E+00	-43.2E+00	73.0E+05	11.6E+00	32.2E-01	12.1E+03	20.1E+03
-5.80E-02	-13.7E+00	-45.1E+00	72.4E+05	11.9E+00	33.0E-01	10.4E+03	22.6E+03
-6.00E-02	-14.1E+00	-47.1E+00	71.8E+05	12.3E+00	34.3E-01	87.5E+02	25.6E+03
-6.20E-02	-14.6E+00	-49.1E+00	71.2E+05	13.0E+00	36.1E-01	70.8E+02	29.0E+03
-6.40E-02	-15.1E+00	-51.2E+00	70.5E+05	13.8E+00	38.3E-01	54.1E+02	32.8E+03
-6.60E-02	-15.5E+00	-53.5E+00	69.7E+05	14.7E+00	40.9E-01	37.5E+02	37.2E+03
-6.80E-02	-16.0E+00	-55.8E+00	68.9E+05	15.8E+00	44.0E-01	20.9E+02	41.9E+03
-7.00E-02	-16.5E+00	-58.3E+00	68.0E+05	17.1E+00	47.6E-01	43.3E+01	47.1E+03
-7.20E-02	-16.9E+00	-61.0E+00	67.1E+05	18.6E+00	51.6E-01	-12.2E+02	52.9E+03
-7.40E-02	-17.4E+00	-63.9E+00	66.0E+05	20.2E+00	56.3E-01	-28.7E+02	59.2E+03
-7.60E-02	-17.9E+00	-67.2E+00	64.9E+05	22.2E+00	61.6E-01	-45.1E+02	66.2E+03
-7.80E-02	-18.4E+00	-70.9E+00	63.5E+05	24.5E+00	68.0E-01	-61.5E+02	74.2E+03
-8.00E-02	-18.8E+00	-75.6E+00	61.8E+05	27.3E+00	76.0E-01	-77.9E+02	83.8E+03
-8.20E-02	-19.3E+00	-82.6E+00	59.2E+05	31.8E+00	88.4E-01	-94.2E+02	97.8E+03

(B) Decelerating cavity

ANNEX

Test results

A prototype amplifier was first tested on a terminating load. The 50 Ω load is transformed via λ/4 coaxial lines to 16 Ω for CW and 8 Ω for pulsed operation. The following results have been obtained at 200 MHz:

	CW operation	pulsed operation pulse length 1s duty cycle 20%
anode voltage	10 kV	10 kV
anode quiescent current	0.5 A	0.5 A
anode current	9.4 A	17.0 A
screen grid voltage	900 V	900 V
screen grid curent	320 m A	405 m A
control grid voltage	-200 V	-200 V
control grid current	105 mA	780 mA
filament voltage	12 V	12 V
filament current	180 A	180 A
RF output power	62 kW	114 kW
RF drive power	1.8 kW	5.2 kW
gain	15.4 dB	13.4 dB
anode efficiency	>64%	>64%
$P_0 = I_{A0} * U_0$	94 kW	170 kW
$P_A = P_0 - P_{RF}$	32 kW	56 kW
$\hat{I}_1 = I_0/f_0 = I_0/0.278$	33,81 [A]	61,15 A
$I_1 = \frac{2P}{U} = \frac{2P}{8.5E3}$	14,588 [A]	26,824 [A]
$R_{RF} = U_{RF}/I_1$	582,66	316,89
$f_1 = \frac{I_1}{\hat{I}_1}$	0,431	0,43866
Hyp 1: $f_0 = 0.278$, $U_{RF} = 8.5$ kV		
$P = \frac{I_1^2 \cdot R}{2} \rightarrow I_1 = \sqrt{\frac{2P}{R}}$	14,376 [A]	27,568 [A]
$U_1 = \frac{2P}{I_1}$	8,625 [kV]	8,27 [kV]
$\hat{I}_2 = \frac{I_1}{f_1} = \frac{I_1}{0.457}$	31,457 [A]	60,32 [A]
Hyp 2: $R = 600\,\Omega$, $f_1 = 0.457$		Hyp 2: $R = 300$, $f_1 = 0.45$

APR 6 1993